CWE-8
June 7-11, 2026
London, ON, Canada

Advances in CFD-based fluid–structure interaction research for engineering structures

Qingshan Yang [a,b], Tian Li [a,b], Feixin Chen [a,b], Yuhao Zhang [a,b]

[a]*School of Civil Engineering, Chongqing University, Chongqing 400045, China*
[b]*State Key Laboratory of Safety and Resilience of Civil Engineering in Mountain Area, Chongqing 400045, China*

SUMMARY

This study develops an advanced CFD-based framework for high-fidelity fluid-structure interaction simulations of engineering structures. To address the key challenges of numerical accuracy and stability under large deformations, the methodology combines high-precision fluid-domain techniques, including structured meshing, a synthetic turbulence inflow method, and internal pressure modelling, with robust dynamic mesh update algorithms such as sliding mesh and spring smoothing dynamic mesh technique. Furthermore, an energy transfer-based post-processing analysis is introduced to elucidate FSI mechanisms by identifying self-excited energy components. The validated framework is successfully applied to simulate complex FSI behaviours in cylindrical structures, wind turbines, and membrane structures, demonstrating its capability to deliver both computationally stable and physically insightful predictions for a range of engineering applications.

Keywords: *fluid-structure interaction, dynamic mesh algorithms, post-processing analysis, engineering structures*

1. GENERAL INSTRUCTIONS

CFD-based numerical simulation is a crucial approach for studying fluid-structure interaction (FSI), yet its application to engineering structures remains constrained by several persistent challenges (Yang et al., 2024). FSI involves tightly coupled multi-physics fields, where local errors readily propagate across domains, imposing stringent accuracy requirements. These difficulties are exacerbated in streamlined structures, such as cylinders (Li et al., 2021), wind turbines (Zhang et al., 2024), and membranes (Yang et al., 2024), characterized by unstable and hard-to-resolve flow separation, complex incoming turbulence, and internal pressure variations, all of which complicate error control in the fluid domain. On the other hand, large structural deformations further induce continuous boundary motion, leading to severe mesh distortion in near-wall regions. This often triggers local error amplification and numerical divergence, making stability under large deformation one of the central technical obstacles. Owing to the absence of high-fidelity and robust dynamic mesh techniques for strongly deforming boundaries, existing studies (Glück et al., 2001; Halfmann et al., 2002; Wu et al., 2008; Sun et al., 2012) commonly simplify the fluid or structural models to maintain stability, at the cost of reduced predictive accuracy. Furthermore, theoretical frameworks for post-processing synchronized flow-structure data remain underdeveloped, limiting mechanistic understanding of FSI phenomena in engineering structures.

In response to these challenges, this study develops high-accuracy CFD methodologies for controlling fluid-domain errors and robust dynamic mesh update algorithm suited to large boundary deformations, thereby enhancing numerical stability. These advances enable an FSI framework that simultaneously ensures computational accuracy and numerical stability. An energy transfer based post-processing method is further proposed to elucidate FSI mechanisms. The overall methodology is successfully applied to cylinders, wind turbines, and membrane structures,

delivering high-fidelity simulations and improved insight into complex FSI behaviors in engineering structures.

2. HIGH-ACCURACY CFD METHODOLOGIES FOR FSI SIMULATION

The accuracy of flow simulations around flexible engineering structures is jointly governed by mesh quality, inflow turbulence characteristics, and the treatment of internal flow fields. To address these issues, a combination of high-fidelity mesh generation method, synthetic turbulence inflow techniques, and internal-flow modeling strategies are developed in this section to enhance reliability and predictive accuracy.

2.1. Structured Meshing Method

To ensure high mesh quality in the fluid domain, a fully structured meshing strategy with localized refinement near solid boundaries is employed. Taking the wind turbine structure as an example, as can be seen in ***Figure 1***, multiple layers of refined meshes are arranged within the boundary layer, while the height of the first-layer cells is strictly controlled according to the target wall y^+ value. This allows accurate resolution of flow separation, reattachment, and vortex shedding on the structural surface during fluid-structure interaction. Meanwhile, a gradual mesh growth rate is applied in the direction away from the structure, enabling a smooth transition from the near-wall refined region to the far field. This strategy balances high near-wall resolution with overall computational efficiency and significantly improves the accuracy of the flow-field solution.

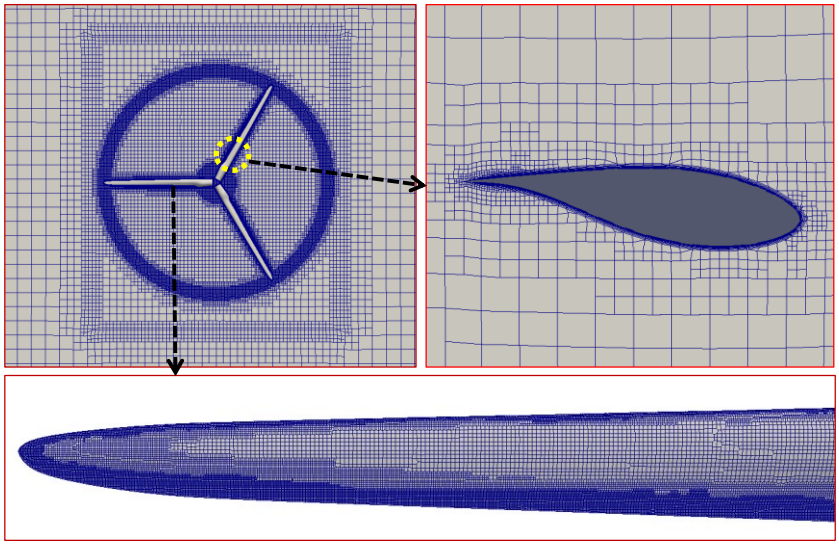

Figure 1: Fluid mesh generation technique.

2.2. Inflow Turbulence Synthesis Technique

Aside from the mesh arrangement, accurate representation of incoming inflow turbulence is also a critical challenge that strongly affects the fidelity of flow-field simulations. Traditional passive approaches, such as roughness elements and grill-based physical modeling are generally unsuitable for FSI simulations. These methods significantly increase the computational cost of the fluid domain beyond the acceptable range for FSI, and they introduce additional numerical errors that accumulate during coupling, thereby degrading overall accuracy.

To overcome these limitations, active inflow turbulence generation techniques based on stochastic-sequence synthesis have been adopted in FSI simulations. The core idea is to discretize the target wind velocity power spectrum and apply a random flow generation (RFG) method to produce fluctuating velocity components for each discrete spectral band. Since this approach can accurately represent the spatial coherence of turbulent flow fields, the coherent-driven RFG (CDRFG) method has been widely used in FSI applications. In this method, the synthesized fluctuating velocity u_i is expressed as:

$$u_i(x_j,t)=\sum_{m=1}^{M}\sum_{n=1}^{N}[p_i^{m,n}\cos(k_j^{m,n}\tilde{x}_j^m+2\pi f_{n,m}t)+q_i^{m,n}\sin(k_j^{m,n}\tilde{x}_j^m+2\pi f_{n,m}t)] \tag{1}$$

$$p_i^{m,n}=\mathrm{sgn}(r_i^{m,n})\sqrt{\frac{2}{N}S_{ui}(f_m)\Delta f\frac{(r_i^{m,n})^2}{1+(r_i^{m,n})^2}};\ q_i^{m,n}=\mathrm{sgn}(r_i^{m,n})\sqrt{\frac{2}{N}S_{ui}(f_m)\Delta f\frac{1}{1+(r_i^{m,n})^2}} \tag{2}$$

here, M denotes the number of discretized spectra; N is the number of random frequencies; $f_{n,m}$ denotes a normally distributed random variable with zero mean and standard deviation f_m; $kmn\ j$ is a random unit vector on a spherical surface; $S_{ui}(f_m)$ represents the velocity spectrum on direction I at frequency f_m; $rm,n\ i$ is a standard normal variable; Δf is the bandwidth of the discrete spectrum; and x_j is the spatial coordinate in direction j.

2.3. Internal Pressure modeling method

For flexible engineering structures with enclosed internal cavities, accurate modeling of the internal flow domain is essential for achieving reliable FSI simulations. Structural vibrations induce boundary deformation, which alters the internal volume and consequently modifies the internal pressure load. Capturing this pressure variation accurately, particularly the pressure-scaling effect introduced by numerical model scaling, is critical for ensuring the fidelity of FSI simulations.

To achieve accurate representation of internal pressure effects, a method based on explicit modeling of the internal flow domain has been developed to directly simulate the internal pressure. Taking an enclosed tensioned-membrane structure as an example, the internal flow domain is explicitly modeled, and, based on the length and wind-speed scaling ratios of the numerical model, a theoretical expression for the internal volume scaling ratio is derived from the equation of state:

$$\lambda_V=\lambda_L{}^3/\lambda_U{}^2 \tag{3}$$

where λ_V is the volume scaling ratio, λ_L and λ_U and are the length and wind velocity scaling ratios, respectively. Using this scaling relationship, the internal volume of the numerical model s adjusted to ensure accurate simulation of internal pressure effect, as illustrated in ***Figure 2***.

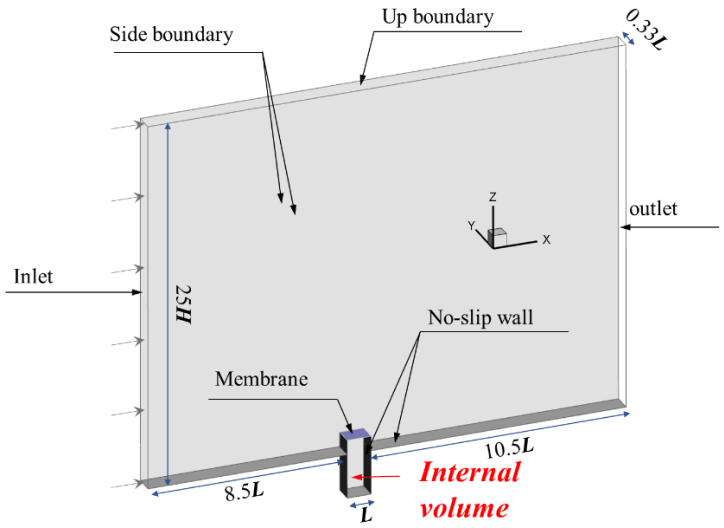

Figure 2: Modelling of internal pressure of closed-type tension membrane structure.

3. DYNAMIC MESH UPDATE ALGORITHMS

To address the challenges of maintaining mesh quality under large deformations in FSI simulations, particularly the difficulty of preserving near-wall mesh quality and ensuring numerical stability, advanced dynamic mesh update algorithms have been developed, which includes sliding mesh techniques and spring-based smoothing methods.

3.1. Sliding Mesh Technique

For FSI scenarios involving large rigid-body displacements of structures, such as cylindrical towers or bridge sections, special treatment is required at the interface between moving and stationary domains. The sliding mesh technique is employed to simulate such cases. The core principle involves using a rotating reference frame formulation in the moving domain while applying a fixed reference frame formulation in the stationary domain. An "information bridge" is established at the interface between the rotating and stationary regions to exchange physical variables, such as velocity and pressure, bi-directionally, as illustrated in ***Figure 3***.

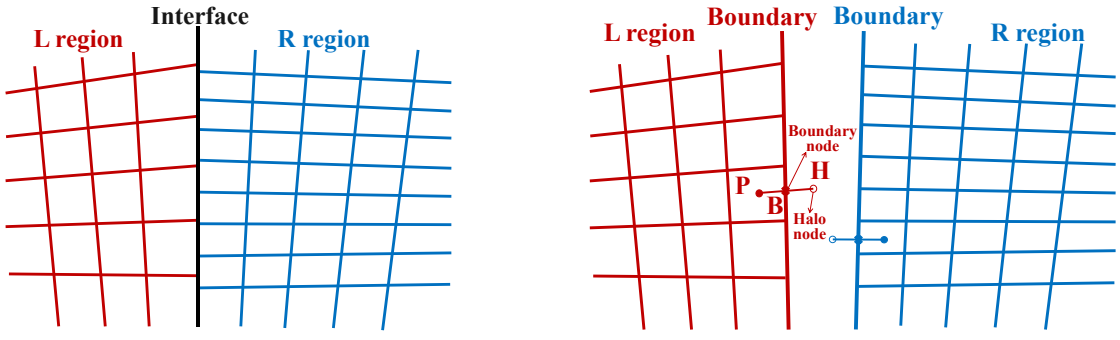

(a) Before deformation

(b) After deformation

Figure 3: Dynamic mesh update using sliding mesh technique.

This procedure employs geometric projection and weighted interpolation methods. For the purposes of geometric projection and overlap computation, the boundary meshes of the rotating and stationary regions are defined as the source face and target face, respectively. First, both meshes are mapped onto a common projection plane, and the overlapping area between the source and target faces is computed. The overlapping area serves as the key basis for transferring physical variables, directly determining the interpolation weights. During the interpolation process, physical variables are transferred between the rotating and stationary regions using weighted interpolation. To ensure the conservation of physical quantities—such as mass and momentum—across the interface, the sliding mesh strictly constrains variable transfer during interpolation. Although this method is not rigorously conservative in the strict sense, since the variables rather than fluxes are directly transferred at the interface, numerical experiments indicate that the resulting error in mass flow is generally negligible.

3.2. Spring Smoothing Dynamic Mesh Technique

For FSI scenarios involving large flexible deformations, such as membrane structures or wind turbine blades, the structural domain's flexible motion can induce substantial changes in the flow-field boundaries, causing severe mesh distortion near walls and potentially leading to numerical divergence. To address this challenge, a smoothing-based dynamic mesh technique has been developed to maintain high-quality near-wall meshes under large-deformation conditions.

The core idea of this method is a spring-based mesh smoothing approach grounded in Hooke's law. Flow-field mesh nodes are treated as interconnected by virtual springs, and the displacement of each mesh node at a given time step can be calculated as:

$$\Delta x_b^{m+1} = \sum_b^{n_a} k_{ab} \Delta x_a^m / (\sum_b^{n_a} k_{ab}) \tag{4}$$

$$k_{ab} = 1/\sqrt{|x_a - x_b|} \tag{5}$$

where Δx represents the mesh displacement; subscripts a and b denote different nodes; k_{ab} is the spring stiffness between nodes and; a and b the superscript m indicates the time step index.

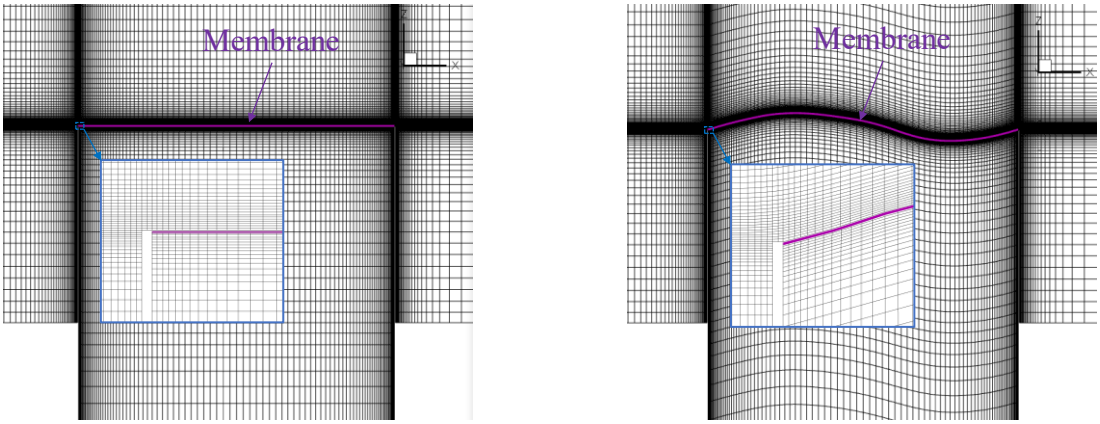

(a) Before deformation (b) After deformation

Figure 4: Dynamic mesh update using spring smoothing technique.

Taking a membrane structure as an example, as can be seen in ***Figure 4***, the mesh nodes within the flow field move following the membrane surface, while the number of nodes and their connectivity remain unchanged. By adjusting the spring stiffness distribution across different regions of the flow field, large deformations near the structure can be effectively transferred to regions farther away, where their impact is minimal. This approach enables high-quality mesh updates in the near-wall region under large structural deformations and significantly improves the numerical stability of coupled FSI simulations.

4. POST-PROCESSING FSI ANALYSIS

Based on the synchronized flow-field and structural-field data obtained form FSI simulation, a post-processing methodology for FSI mechanisms is developed in this section, which integrates energy analysis and coherence analysis.

First, using synchronized wind-load and structural displacement data, the generalized equation of motion for the structure during FSI process can be formulated as:

$$M_{Gj}\ddot{d}_{Gj}(t)+C_{Gj}\dot{d}_{Gj}(t)+K_{Gj}d_{Gj}(t)=F_{Gj}(t,d_{Gj},\dot{d}_{Gj},\ddot{d}_{Gj}) \tag{6}$$

where M_{Gj}, C_{Gj}, K_{Gj} and denote the generalized mass, damping, and F_{Gj} stiffness of the membrane structure corresponding to its -th mode, respectively, and represents the external load. Considering FSI effects, the external load is a function of both time and structural motion. Based on the generalized degrees of freedom, load–displacement hysteresis analysis is employed to evaluate energy transfer during the coupled process, as illustrated in ***Figure. 5***.

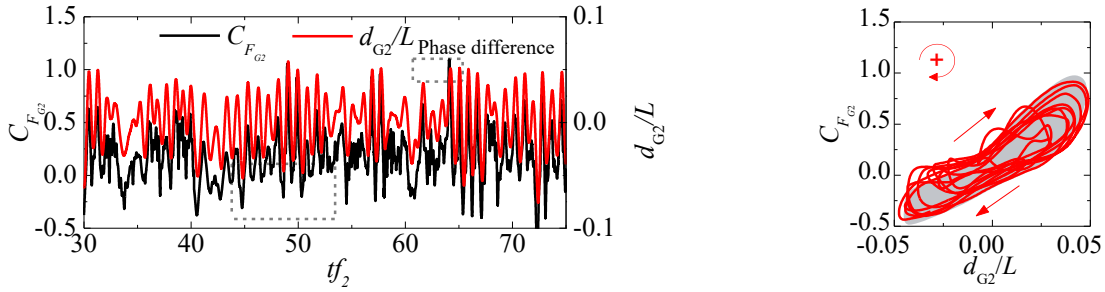

(a) Synchronized wind force and displacement

(b) Hysteresis loop

Figure 5: Hysteresis analysis between wind load and displacement.

Additionally, using a simplified aero-elastic model and a load–displacement orthogonal decomposition method, a technique for identifying self-excited energy in the coupled process is established. The influence of self-excited energy is represented as additional terms related to the structural properties. The simplified aero-elastic equation can thus be expressed as:

$$M_{Gj}\ddot{d}_{Gj}(t)+(C_{Gj}+C_{aj})\dot{d}_{Gj}(t)+(K_{Gj}+K_{aj})d_{Gj}(t)=F_{Wj}(t) \tag{7}$$

where *Caj* and *Kaj* denotes the aerodynamic damping and stiffness, representing the components of self-excited energy associated with velocity and displacement, respectively. By substituting the synchronized load-displacement data obtained from simulations into the energy conservation

equation, the characteristics of self-excited energy during the coupled process can be determined, as:

$$K_{aj} = \frac{\int_0^{nT} F_{Gj}(t) d_{Gj}(t) dt}{-\int_0^{nT} d^2{}_{Gj}(t) dt} \tag{8}$$

$$C_{aj} = \frac{\int_0^{nT} F_{Gj}(t) \dot{d}_{Gj}(t) dt}{-\int_0^{nT} \dot{d}^2_{Gj}(t) dt} \tag{9}$$

Taking tension membrane structure as an example, with the above theory, the identified non-dimensional aerodynamic damping ratio and aerodynamic stiffness ratio are described in ***Figure 6***.

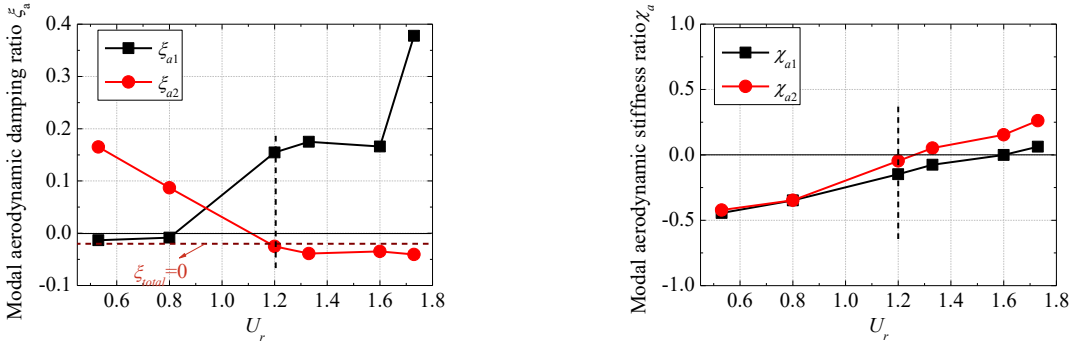

(a) Aerodynamic damping ratio

(b) Aerodynamic stiffness ratio

Figure 6: Analysis of self-excited energy.

5. APPLICATION OF DEVELOPED FSI SIMULATION METHOD

The numerical FSI techniques developed above have been successfully applied to cylindrical structures, tensioned-membrane structures, and wind turbine systems, achieving high-fidelity reproduction of their respective FSI responses, as illustrated in Fig. 7. Figure 7(a) shows the simulated cross-wind vibration of a flexible cylindrical structure, where pronounced FSI-induced oscillations are observed. Figure 7(b) presents the FSI behavior of an enclosed tension membrane structure, in which significant membrane deformation occurs, and the internal-pressure effects during coupling are accurately captured through internal flow-domain modeling. Figure 7(c) depicts the wake vortex field of a wind turbine, simulated with both blade rotational motion and platform rigid-body motion taken into account. Figure 7(d) illustrates the numerical reproduction of the FSI process for a floating platform, including the evolution of the free surface under wave excitation.

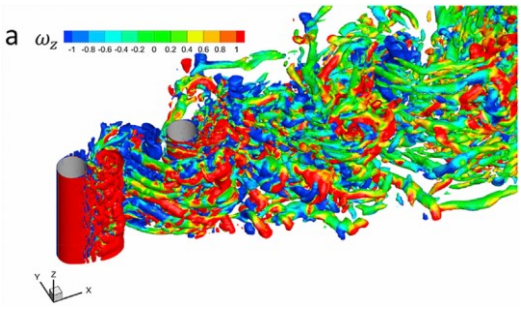

(a) Cylindrical structure

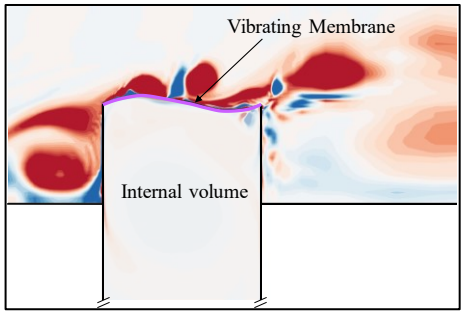

(b) Tension membrane structure

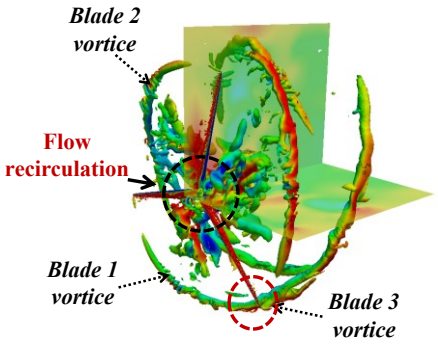

(c) Blade of wind turbine

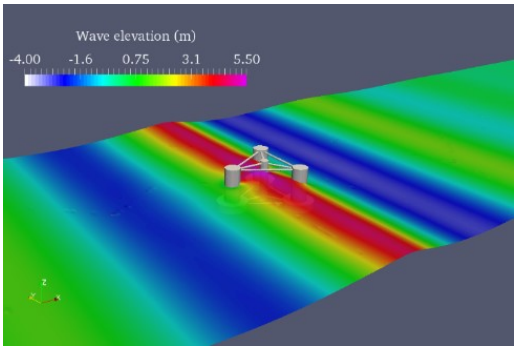

(d) Floating platform of wind turbine

Figure 5: Application of FSI simulation technique

6. CONCLUSION

This study successfully establishes a high-fidelity and robust numerical framework for simulating complex fluid-structure interaction (FSI) in engineering structures. The developed methodology encompasses high accuracy CFD techniques including structured meshing and synthetic turbulence generation to ensure precise flow resolution. For handling structural motions, advanced dynamic mesh algorithms comprising sliding mesh for rigid body motion and spring smoothing for flexible deformations effectively maintain mesh quality. The proposed energy transfer based post processing method provides a profound mechanistic understanding of complex FSI phenomena by quantitatively identifying self excited energy components. Comprehensive validations through applications to cylindrical structures, wind turbines and membrane systems demonstrate the framework's robustness and general applicability for simulating complex FSI phenomena in engineering practice, representing a significant advancement beyond conventional simplified approaches.

REFERENCES

Glück, M., Breuer, M., Durst, F, et al. 2001. Computation of fluid-structure interaction on lightweight structures. J. Wind Eng. Ind. Aerodyn. 89(14-15): 1351-1368

Halfmann, A., Rank, E. Glück, M. et al, 2002. Computational engineering for wind-exposed thin-walled structures. Lecture Notes in Computational Science and Engineering. Berlin: Springer: 63-70

Li, T., Takeshi, I., 2021. Numerical study on vortex-induced vibration of circular cylinder with two-degree-of-freedom and geometrical nonlinear system, Journal of Fluid and Structures. 107, 103415

Sun, X.Y., Wu, Y., Chen, Z.Q., 2012. CFD numercical simulation on wind structure interation of membrane structures.

Chinese journal of Computaional Mechanics
Yang, Q.S., Chen, F.X., et al., 2024. Fluid-structure interaction behaviors of tension membrane roofs by fully-coupled numerical simulation. J. Wind Eng. Ind. Aerodyn.244: 105609
Wu, Y., et al., 2008. Computation of wind-structure interaction on tension structures[J]. Journal of Wind Engineering and Industrial Aerodynamics. J. Wind Eng. Ind. Aerodyn. 96(10): 2019-2032